Fast-neutron-induced fission of ^{242}Pu at *n*ELBE

Toni Kögler[1,2,a], Roland Beyer[1], Mirco Dietz[1,2], Arnd R. Junghans[1,b], Christian Lorenz[2,c], Stefan E. Müller[1], Tobias P. Reinhardt[2], Konrad Schmidt[1,2,d], Ronald Schwengner[1], Marcell P. Takacs[1,2], and Andreas Wagner[1]

[1] Helmholtz-Zentrum Dresden - Rossendorf, Postfach 510 119, 01314 Dresden, Germany
[2] Technische Universität Dresden, Postfach 100 920, 01076 Dresden, Germany

Abstract. The fast neutron-induced fission cross section of ^{242}Pu was determined in the range of 0.5 MeV to 10 MeV relative to ^{235}U(n,f) at the neutron time-of-flight facility *n*ELBE. The number of target nuclei was calculated by means of measuring the spontaneous fission rate of ^{242}Pu. Neutron transport simulations with Geant4 and MCNP6 are used to correct the relative cross section for neutron scattering. The determined results are in good agreement with current experimental and evaluated data sets.

1. Introduction

Neutron-induced fission cross sections of actinides such as the Pu-isotopes are of relevance for the development of nuclear transmutation technologies. Apart from ^{244}Pu, whose abundance in spent nuclear fuel could be neglected [1], ^{242}Pu is the plutonium isotope with the longest half-life ($T_{1/2} = 373300$ a). Thus, there is a special interest to investigate the fission of this particular isotope using fast neutrons.

The fast neutron-induced fission cross section of ^{242}Pu was studied first by Butler in 1960 [2]. A brief summary of the available experimental data acquired since then is given in Ref. [3]. Results of measurements at the Los Alamos National Laboratory by Tovesson et al. [4] and at the Joint Research Center Geel by Salvador-Castiñeira et al. [3] were published recently and tend to be lower than present evaluated nuclear data [5].

For ^{242}Pu(n,f) current uncertainties are of about 21% in an energy range of 0.5–2.23 MeV. Sensitivity studies [6,7] show that the total uncertainty has to be reduced to below 5% to allow for reliable neutron physics simulations of plutonium using reactor concepts.

This challenging task was performed at the neutron time-of-flight facility *n*ELBE of the Center for High-Power Radiation Sources ELBE at Helmholtz-Zentrum Dresden – Rossendorf. Improved experimental conditions (low scattering environment) and beam power, paired with the right spectral shape of the neutron source provide excellent conditions to achieve this aim.

The present work reports an experiment at *n*ELBE studying the neutron-induced fission cross section of ^{242}Pu relative to ^{235}U(n,f).

[a] e-mail: t.koegler@hzdr.de
[b] e-mail: a.junghans@hzdr.de
[c] Present address: Lund University, PO Box 117, 221 00 Lund, Sweden
[d] Present address: National Superconducting Cyclotron Laboratory, Michigan State University, East Lansing, Michigan 48824, USA

2. Experiments

2.1. Fast neutrons at ELBE

At *n*ELBE fast neutrons between 10 keV and 20 MeV are generated by a photo-neutron source. Impinging electrons of the ELBE beam produce bremsstrahlung while getting decelerated in a liquid lead target [8]. Neutrons are further produced via (γ, n) reactions on the lead nuclei. The compactness of the neutron producing target together with the excellent timing of the ELBE electron beam enables high resolution neutron time-of-flight experiments even at short flight paths of around 6 m. Further details of *n*ELBE can be found in Ref. [9]. For this experiment a repetition rate of 406.25 kHz was chosen as a compromise between avoiding pulse overlap and maximum beam intensity. The electron beam energy was 30 MeV and the average bunch charge 73 pC.

2.2. Fission chambers

Within the TRAKULA project [10], large and homogeneous deposits of ^{235}U and ^{242}Pu have been produced successfully [11]. Two fission ionization chambers, one assembled with uranium (UFC) and one with plutonium (PuFC), have been constructed and built at HZDR [12,13]. In the reported experiment only the PuFC was used. The incident neutron flux was determined with the well characterized transfer device H19 of the PTB Braunschweig [14,15], which is also an ^{235}U fission chamber. Both fission chambers were operated in the forward biasing mode, which means that the five double-sided fission samples of the H19 and the eight sin-gle–si-ded samples of the PuFC are cathodes on positive potential. The induced charge on the anode was read out by a nanosecond preamplifier developed in-house.

2.3. Data acquisition

The short signal length of the ns-preamplifier reduces the α-pile-up probability by nearly a factor of 5 compared to conventional μs-shaping time preamplifiers. In addition

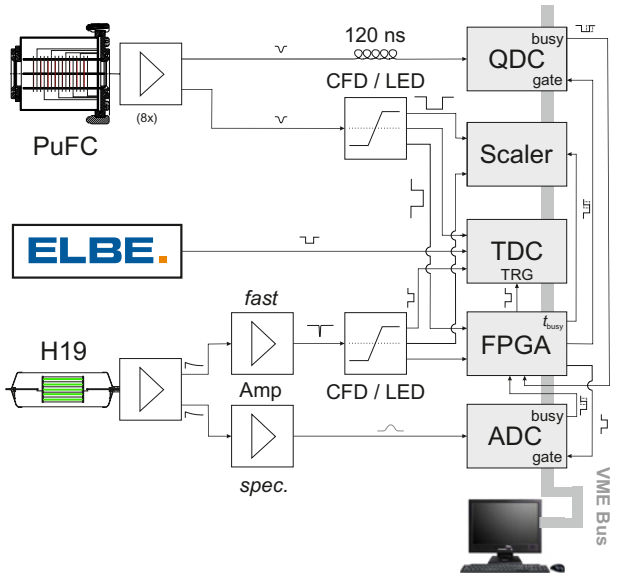

Figure 1. Scheme of the electronic setup and the data acquisition system. The output signals of the charge-sensitive (ns-) preamplifiers are split to determine the timing and the collected charge. The pulse heights of the H19 signals are acquired with an ADC after getting shaped by a spectroscopic amplifier, whereas the charge of the eight PuFC channels (only one is shown here) is determined by a QDC. The second output signal is converted to a logical signal by an in-house developed constant fraction discriminator (CFD). The production of a fast trigger makes the use of a timing-filter-amplifier in the fast branch of the H19 necessary. The logical signals are used to determine the timing in a time-to-digital converter (TDC) and to produce a trigger for the data acquisition in an FPGA.

it enables the use of a charge-to-digital converter (QDC) instead of the combination of a spectroscopic amplifier and an analog-to-digital converter (ADC). A scheme of the VME-based data acquisition electronics is shown in Fig. 1. Further details of the used experimental setup and electronics can be taken from Ref. [16].

2.4. Data analysis

The recorded list-mode data were analyzed using the Qt/ROOT-based software framework Go4 [17]. The produced time-of-flight spectra (cf. Fig. 2) were calibrated with respect to the bremsstrahlung peak. A gate on the QDC values was applied to filter out the α-particle background coming from the radioactive decay of the target nuclei. Time-independent fission events caused by room-return background and spontaneous fission were approximated by a constant in front of the bremsstrahlung peak, between this peak and the begin of the neutron-induced fission events and at the end of the spectrum.

Both, time-of-flight spectrum and background were translated into kinetic energy by using Eq. (1).

$$E_n(t) = m_n c^2 \left(\frac{1}{\sqrt{1 - \left(\frac{L}{tc}\right)^2}} - 1 \right), \qquad (1)$$

where $m_n c^2$ stands for the neutron rest energy, L for the flight path and t for the time-of-flight of the neutron to a certain actinide target.

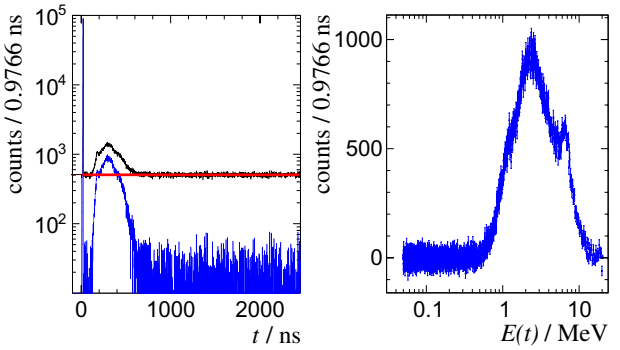

Figure 2. Left: neutron time-of-flight spectrum acquired by one channel of the plutonium fission chamber before (in black) and after (in blue) background subtraction. The red line indicates a constant extrapolation of the background induced by room-returned neutrons and spontaneous fission events. Right: background subtracted energy spectrum calculated using the time-of-flight spectrum shown on the left side.

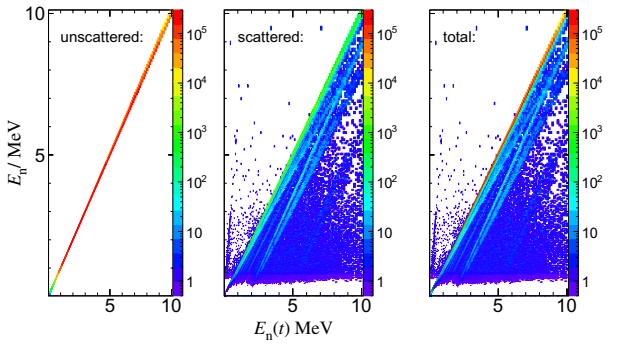

Figure 3. Simulated energy to time-of-flight-correlation calculated using Geant4. Shown are from left to right: unscattered neutrons, scattered neutrons and the sum of both. Here the bin content was multiplied columnwise with the ^{242}Pu fission cross section.

After background subtraction the relative fission cross section can be calculated by:

$$\frac{\sigma^{\mathrm{PuFC}}_{(\mathrm{n,f})}}{\sigma^{\mathrm{H19}}_{(\mathrm{n,f})}} = K \frac{\sum_i \left(C\varepsilon \dot{N}_{(\mathrm{n,f})}\right)^{\mathrm{PuFC}_i}}{\langle C \rangle^{\mathrm{H19}} \sum_i \left(\varepsilon \dot{N}_{(\mathrm{n,f})}\right)^{\mathrm{H19}_i}}. \qquad (2)$$

Here $\dot{N}_{(\mathrm{n,f})} = \dot{N}_{(\mathrm{n,f})}(E_n(t))$ is the detected neutron-induced fission rate at a certain time-of-flight t in the i-th actinide target of the PuFC or the H19. This count rate has to be corrected for the fission fragment detection efficiency ε and for neutron scattering C, which will be discussed in Sect. 2.5.

The normalization factor K is the ratio of the total areal densities n_A of the two fission chambers and depends only on constants.

Because ^{242}Pu has a high spontaneous fission (SF) rate $\lambda\gamma$, which is in addition known better than 2% (see Ref. [18, 19]), n_A^{PuFC} can be determined by measuring the spontaneous fission rate $\dot{N}_{(\mathrm{SF})}$. As the target area F^{PuFC_i} is equal for all eight deposits this simplifies to a sum over the effective areal density of each actinide target:

$$n_A^{\mathrm{PuFC}} = \sum_i n_A^{\mathrm{PuFC}_i} = \frac{1}{\lambda\gamma F} \sum_i \left(\alpha\varepsilon \dot{N}_{(\mathrm{SF})}\right)^{\mathrm{PuFC}_i} \qquad (3)$$

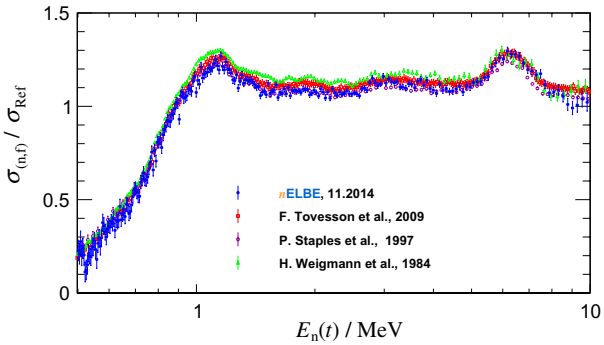

Figure 4. Neutron-induced-fission cross section of ^{242}Pu relative to ^{235}U. The *n*ELBE data are shown in blue together with selected EXFOR-data of Tovesson et al. [4], Staples et al. [22] and Weigmann et al. [20]. Within their uncertainties there is a good agreement of the presented data set with the data of Staples and Tovesson. Small deviations from the re-normalized (ENDF/B-V→ ENDF/B-VII.1) Weigmann data are clearly visible.

Here α accounts for the small dead time correction of the DAQ during this measurement. With Eq. (3) the normalization factor can be written as follows:

$$K = \frac{\lambda\gamma F n_A^{\mathrm{H19}}}{\sum_i \left(\alpha\varepsilon\dot{N}_{(\mathrm{SF})}\right)^{\mathrm{PuFC}_i}}. \tag{4}$$

Using this expression in Eq. (2), the relative cross section gets independent from the fission fragment detection efficiency of the PuFC, which is usually difficult to determine [20]. Of course one has to correct for the linear and angular momentum introduced by the incident neutrons. Subsequently to this momentum transfer an anisotropy in the emission of the fission fragments arise, which lowers the detection efficiency [21]. Due to the lack of experimental data for this anisotropy, this inefficiency was not corrected for. An estimation of this measure was done using unpublished data of Salvador-Castiñeira et al. and included to the systematic uncertainties.

2.5. Neutron scattering corrections

To correct for the influence of neutron scattering one has to consider two different aspects. The first is the attenuation of the neutron beam by passing any material along its track. The second is the loss of the energy to time-of-flight correlation of scattered neutrons. Especially for inelastic scattered neutrons this is an important issue, because they are losing a large amount of their total kinetic energy in one interaction. Measuring their time-of-flight afterwards will lead to a much higher kinetic energy, if the scattering was close to the fission targets. As a result of that, the cross section at high energy would be overestimated.

Both effects have been corrected for using an MCNP 6.1.1 and a Geant 4.10.1 simulation. The results of both neutron transport codes were in a very good agreement to each other. The outcome of the simulation is a correlation matrix of the true kinetic energy E_n and the kinetic energy $E_n(t)$ one would calculate from their time-of-flight and the assumed undisturbed flight path. For the Geant 4 simulation such a correlation matrix for an arbitrary actinide target is shown in Fig. 3.

The attenuation of the neutron beam was corrected by the ratio of all impinging neutrons N^i in the i-th actinide target, which have not been scattered on their way to the target (on the left of Fig. 3), to the total number of started neutrons N^0. Hence one could define a transmission correction factor T up to the target i as:

$$T^i(E_n(t)) = \frac{N^i(E_\mathrm{n} = E_n(t))}{N^0} \tag{5}$$

The loss of the energy to time-of-flight correlation could be expressed in a similar way. Here the correction factor k^i is the ratio of the detected fission rate of unscattered neutrons to the total detected fission rate. Because the fission rate depends on the cross section, the results of the simulations were multiplied by the JEFF 3.2 evaluated fission cross section of ^{242}Pu:

$$k^i(E_n(t)) = \frac{\int N^i(E_n^{'}, E_n(t))\sigma(E_n^{'})\delta(E_n^{'} - E_n(t))\mathrm{d}E_n^{'}}{\int N^i(E_n^{'}, E_n(t))\sigma(E_n^{'}))\mathrm{d}E_n^{'}} \tag{6}$$

The delta-distribution $\delta(E_n^{'} - E_n(t))$ in the numerator ensures that only unscattered neutrons are taken into account. With Eq. (5) and Eq. (6) the neutron scattering correction factor C^i is defined in the following way:

$$C^i = \frac{k^i}{T^i} \tag{7}$$

As only the sum of all H19 fission targets is available, the arithmetic mean $\langle C\rangle^{\mathrm{H19}}$ was calculated to take care of the neutron scattering within this chamber. Then, the average total correction factor is in the order of 9%.

3. Results

Including the neutron scattering corrections into Eq. (2) one can finally calculate the relative neutron-induced fission cross section of ^{242}Pu. The result of this calculation is shown in Fig. 4.

The *n*ELBE data are in good agreement in shape and absolute scale to present nuclear data. Compared to the data of Staples et al. [22], the accordance in absolute scale is above 99%. The discrepancy to the Tovesson [4] data set is around 2% in the considered energy range. Larger deviations to the Weigmann data [20] in the order of 5.4% are present especially in the plateau region between 1.2 MeV and 5 MeV. The recently published data of Salvador-Castiñeira et al. [3] are also below this cross section ratio. This is of special interest, because the current European evaluation JEFF 3.2 (see Ref. [23]) is mainly based on the Weigmann data.

3.1. Uncertainties

The statistical uncertainty of the presented data ranges from 1.1% in the plateau to ≈ 47% in the threshold and second-chance fission region, where the neutron fluence of *n*ELBE is too low to achieve better statistics within a reasonable measuring time.

The main contribution to the systematic uncertainty is caused by the uncertainty in the normalization factor K ($\sigma_K/K \approx 2.1\%$). If one includes the uncertainty in the reference cross section ($\approx 0.7\%$), the neutron scattering correction (0.21%) and the uncertainty in the fission fragment anisotropy caused by linear and angular momentum transfer (1.6%) one ends up in a total systematic uncertainty of 2.7%.

4. Summary

The fast neutron-induced fission cross section of ^{242}Pu has been measured in the range of 0.5–10 MeV at *n*ELBE. The neutron scattering is a crucial correction which has to be done in neutron time-of-flight experiments. For the described experiment the average scattering correction was around 9%.

The presented data are in good agreement with previous data sets in the threshold region. At the plateau we achieved excellent agreement with the Staples and Tovesson data, but there are deviations from the data of Weigmann et al., which the JEFF 3.2 evaluation is mainly based on. In this energy range we achieved a statistical uncertainty of 1.1%. The average systematic uncertainty is 2.7% caused mainly by the uncertainty in the normalization.

References

[1] A. Schwenk-Ferrero, Science and Technology of Nuclear Installations (2013)
[2] A. Butler, Phys. Rev. **117**, 1305 (1960)
[3] P. Salvador-Castiñeira et al., Phys. Rev. C **92**, 044606 (2015)
[4] F. Tovesson et al., Phys. Rev. C **79**, 014613 (2009)
[5] M. Chadwick et al., Nucl. Data Sheets **112**, 2887 (2011)
[6] Working Party on International Evaluation Co-Operation, OECD / NEA (2008) `http://www.oecd-nea.org/science/wpec/volume26/volume26.pdf`
[7] OECD / NEA, *The Nuclear Data High Priority Request List (HPRL)* `http://www.oecd-nea.org/dbdata/hprl/`
[8] E. Altstadt et al., Ann. Nucl. Energy **34**, 36 (2007)
[9] R. Beyer et al., Nucl. Instr. and Meth. A **723**, 151 (2013)
[10] *Das TRAKULA-Projekt (BMBF 02NUK13A)* `http://www.hzdr.de/db/Cms?pNid=2721`
[11] A. Vascon et al., Appl. Radiat. Isot. **95**, 36 (2015)
[12] T. Kögler et al., Phys. Proc. **47**, 178 (2013)
[13] T. Kögler et al., CERN-Proceedings **2014–002**, 25 (2014)
[14] D.B. Gayther, Metrologia **27**, 221 (1990)
[15] R. Nolte et al., Nucl. Sci. Eng. **156**, 197 (2007)
[16] T. Kögler, Dissertation, Technische Universität Dresden (2016)
[17] J. Adamczewski-Musch et al., *The Go4 Analysis Framework*, GSI `http://web-docs.gsi.de/~go4/go4V05/manuals/Go4introV5.pdf`
[18] N.E. Holden et al., Pure Appl. Chem. **72**, 1525 (2000)
[19] M.M. Bé et al., *Table of Radionuclides*, Vol. **5** (2010), `http://www.bipm.org/en/publications/scientific-output/monographie-ri-5.html` ISBN 92-822-2234-8
[20] H. Weigmann et al., Nucl. Phys. A **438**, 333 (1985)
[21] G. W. Carlson., Nucl. Instr. and Meth. **119**, 97 (1974)
[22] P. Staples et al., Nucl. Sci. Eng. **129**, 149 (1998)
[23] OECD / NEA, *JEFF-3.2 evaluated data library-Neutron data* `https://www.oecd-nea.org/dbforms/data/eva/evatapes/jeff_32/`